



## INTERACTION BETWEEN A MAJOR CRACK AND SMALL CRACK DAMAGE IN AIRCRAFT SHEET MATERIAL

K.-F. NILSSON

The Aeronautical Research Institute of Sweden, Structures Department,  
P.O. Box 110 21, S-161 11 Bromma, Sweden

and

J. W. HUTCHINSON

Division of Applied Sciences, Harvard University, Cambridge, MA 02138, U.S.A.

(Received 20 September 1993; in revised form 9 February 1994)

**Abstract**—A study is made of the effect of small crack damage on the fracture tolerance of an elastic–plastic sheet material to a major crack. The study is motivated by concern for the influence of multiple-site fatigue damage in lap joints on the tolerance of aging aircraft fuselages to major cracks. Flat sheet geometries are analysed, both unreinforced and reinforced. Several analysis approaches are explored and assessed, including linear elastic fracture mechanics (LEFM), a modification of LEFM employing a damage-reduced fracture toughness, and a modification of the Dugdale model which makes use of a damage-reduced yield stress of the sheet material. An important feature of the interaction between a major crack and small crack damage is the fact that the plastic zone of the major crack engulfs at least several damage sites in geometries typical of most lap joint designs. The damage-reduced yield strength of the lap joint emerges as being central to understanding the role of damage, and simple formulas are given which indicate how damage erodes tolerance in the presence of a major crack.

### NOTATION

|                           |  |
|---------------------------|--|
| $L$                       | tear strap half-spacing  |
| $a$                       | half-length of macro-crack   |
| $w$                       | width of tear strap  |
| $n$                       | rivet spacing along the tear straps                                    |
| $t$                       | thickness of sheet and tear straps                                     |
| $R$                       | radius of rivet  |
| $a_{\text{MSD}}$          | small crack half-length representing MSD                               |
| $\sigma$                  | applied stress carried by skin   |
| $\sigma_c$                | applied stress at which major crack advance occurs                     |
| $\sigma_y$                | yield stress of skin   |
| $\sigma_y^{\text{strap}}$ | yield stress of strap  |
| $\bar{\sigma}_y$          | averaged yield stress of skin along line of small MSD cracks           |
| $s$                       | rivet spacing along lap joint  |
| $D_{\text{MSD}}$          | measure of damage due to MSD cracks                                    |
| $d$                       | separation between dislocations in doublet pair                        |
| $K$                       | mode I stress intensity factor of the major crack in the LEFM approach |
| $K_c$                     | mode I toughness of the undamaged skin material                        |
| $\delta_c$                | crack tip opening displacement   |
| $\delta_c^*$              | critical value of crack tip opening displacement for crack advance     |
| $\lambda$                 | length of modified Dugdale zone at major crack tip.                    |

### INTRODUCTION

The fuselage of a modern aircraft combines shell skin, stringers, rings and tear strap reinforcements in a sophisticated manner designed to provide the pressurized fuselage with a tolerance to major cracks. An important issue which has emerged in the international effort to investigate problems associated with the aging fleet of commercial aircraft is to what extent, if any, widespread fatigue damage at rivets in the fuselage lap joints impairs

the tolerance of the fuselage to major lap joint cracks. Pressurization and depressurization cycles associated with each flight have the potential of producing damage in the form of small fatigue cracks emanating from rivet holes along the lap joint. The original assessment of tolerance of pressurized fuselages to major longitudinal cracks was established on the basis of undamaged lap joints. The Aloha Airlines accident in 1988 drove home the fact that small crack fatigue damage could degrade the major crack tolerance of a fuselage. An unusual feature of this damage is the relatively uniform manner in which it has been observed to appear at multiple rivet locations along the lap joint, and this form of widespread fatigue damage is referred to as multiple-site damage (MSD). By the end of this decade more than 50% of the international commercial aircraft fleet will exceed 20 years of age, which places many of the aircraft beyond the lifetime they were designed for, given the expected number of flights per year. There is every reason to expect that aging effects will become an increasing problem, and it is suspected that the damage tolerance methodology for these aircraft may have to be modified to account for MSD.

This paper represents a beginning attack on the problem of the extent to which lap joint MSD reduces the residual strength of an aircraft fuselage in the presence of a major crack. The complexity of the full problem and the large number of parameters involved, render modeling difficult. Simplified models must be relied upon, especially for the purpose of establishing dominant effects. A basic understanding and approach to cracked stiffened sheets and shells has been laid out by Swift (1974, 1986), and applications of fracture mechanics to assess repair strategies is illustrated in Park *et al.* (1992). Recent work on the interaction between a major crack and a few small cracks in flat stiffened sheets has been presented by Tong *et al.* (1994), based on elastic finite element methods. Newman *et al.* (1993) have approached the problem for the unreinforced sheet using a large scale yielding plasticity formulation. They have clearly demonstrated the importance of accounting for plastic yielding, when due recognition is made of representative material properties and crack sizes in the fuselage problem. The importance of understanding the role of plastic yielding emerges as being perhaps the central issue from the present study. The role of plasticity in the fuselage problem can be appreciated when one realizes that the length of the plastic zone at the tip of a long crack in aircraft aluminum sheet material at the onset of crack advance is typically about 2–4 inches, depending on the particular material. The plastic zone of the major crack is therefore large enough to completely engulf at least several rivets, and perhaps more, since the rivet spacing is typically 1 inch. If fatigue damage exists at the rivets, it will necessarily interact with the plastic zone of the major crack. The results of the present paper suggest that the important factor in understanding the interaction of a major crack with MSD is knowledge of the extent to which the MSD reduces the average yield strength of the joint.

The two sets of problems shown in Fig. 1 are modeled and analysed. The first and most straightforward is the macro-crack of length  $2a$  in an infinite sheet where small micro-cracks (these will be thought of as the MSD cracks) lie on either side and along the line of the major crack. The failure analysis of the sheet will be analysed using linear elastic fracture mechanics and, more importantly, by an approach which incorporates plastic yielding ahead of the major crack and between the micro-cracks. Values of the various geometric and material parameters representative of fuselage applications will be chosen so that the method of assessment and development will have relevance to the fracture of lap joints. This problem will be used to assess the approximate elastic–plastic approaches proposed in this paper. The more complicated problem, which contains some of the essential features relevant to crack arrest design of a fuselage lap joint, is shown in Fig. 1(b). Now, two tear straps are riveted or bonded to the flat sheet, and their effect on the residual strength of the flat sheet will be determined as a function of the length  $2a$  of the major crack and the level of MSD damage, which is again modeled by micro-cracks. Here, too, the predictions of an approach based on linear sheet response will be contrasted with those from two elastic–plastic fracture approaches, primarily to bring out the shortcomings of LEFM as applied to this problem. Yielding of the tear straps will be taken into account in all cases. We begin by describing four aspects of the modeling which are common to both sets of problems.

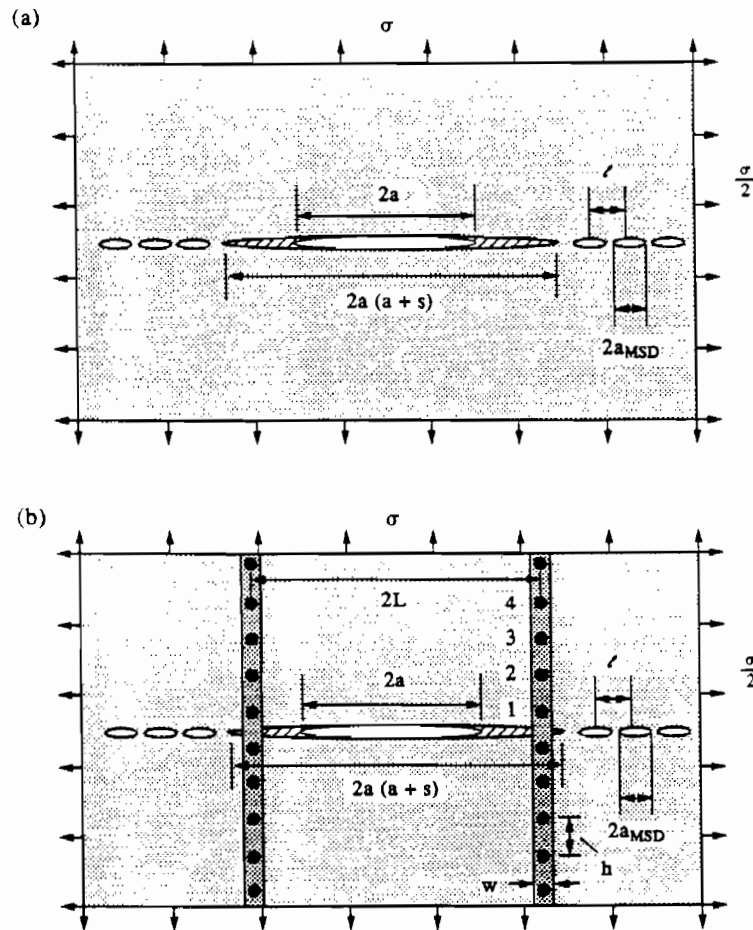


Fig. 1. Model problems: (a) flat unstiffened sheet with a major crack and smaller MSD cracks; (b) flat stiffened sheet with a major crack and smaller MSD cracks.

#### PRELIMINARY MODELING ASPECTS

##### *Fracture criterion in a thin sheet accounting for plastic yielding*

The linear elastic fracture criterion used in this paper will ignore any resistance curve behavior of the sheet material, and it will be assumed that a macro-crack can advance when its stress intensity factor,  $K$ , reaches an effective sheet toughness,  $K_c$ . The elastic-plastic criterion for crack advance, which also ignores growth resistance effects, is based on a critical value of the crack tip opening displacement,  $\delta_t^c$ . In the elastic-plastic formulation, the crack tip opening displacement  $\delta_t$  will be computed and the condition  $\delta_t = \delta_t^c$  will be imposed for predicting the onset of macro-crack advance. In this paper, the sheet material will be modeled as being elastic-perfectly plastic with a tensile yield stress  $\sigma_Y$ . For plane stress in the small scale yielding limit,  $\delta_t = K^2 / (E\sigma_Y)$ . Thus,  $\delta_t^c$  is related to  $K_c$  by

$$\delta_t^c = K_c^2 / (E\sigma_Y). \quad (1)$$

The condition  $\delta_t = \delta_t^c$  pertains in both large and small scale yielding. By virtue of eqn (1), the elastic-plastic approach necessarily reduces to the predictions of linear elastic approach in the small scale yielding limit.

In a recent report Newman *et al.* (1993) also carried out a flat sheet analysis of the interaction between a large crack and smaller MSD cracks. They employed a criterion based on a critical crack tip opening angle, modified in some instances by an additional condition to characterize initiation of growth. Their predictions are based on numerical results from a plane stress finite element model, and they accounted for the strain hardening properties of the sheet material. Their model does predict some resistance curve behavior

for the pristine sheet material. Aircraft aluminum sheet material does generally display *R*-curve behavior. One way or the other, the present approach will have to be extended to accommodate such behavior.

*The reduced average tensile yield stress  $\bar{\sigma}_Y$  of the micro-cracked damaged sheet*

The two parts of Fig. 2 depict how the weakening of the sheet by the micro-cracks (i.e. the MSD damage) is taken into account in the modified Dugdale model. Plastic yielding ahead of a macro-crack in a thin elastic-perfectly plastic sheet is adequately modeled by a Dugdale zone. In the Introduction, it was pointed out that the plastic zone ahead of a major crack at the onset of crack advance in a typical aircraft aluminum sheet material will be at least of the order of 2–4 inches, engulfing at least 2–4 rivets. Any reduction of the ligament area resulting from fatigue cracks growing from the rivet holes will show up as a corresponding reduction in the local plastic limit load capacity of the sheet. The exact details of this reduction are complicated. Here we will imagine, as depicted in Fig. 2(a), that the MSD damage is equivalent to micro-cracks of length  $2a_{\text{MSD}}$ , and our measure of the effect that this damage has on the local plastic limit load stress is represented by a reduced average limit yield stress

$$\bar{\sigma}_Y = \sigma_Y(\ell - 2a_{\text{MSD}})/\ell \equiv \sigma_Y(1 - D_{\text{MSD}}) \quad (2)$$

where  $\ell$  is the center to center spacing of the micro-cracks, i.e. the rivet spacing. Thus,  $D_{\text{MSD}}$  will be our measure of the damage due to the fatigue cracks at the rivet holes. For the micro-cracked sheet, it is precisely the reduction in area fraction of the ligaments. For a riveted joint, this damage parameter reflects the reduction in local yield strength due to the fatigue crack damage. Under the assumption that the plastic zone ahead of the major crack tip spans at least several of the rivets, plastic yielding will be represented by a Dugdale zone with an effective, or average, yield stress  $\bar{\sigma}_Y$ . The length of this zone will be treated as an unknown variable, just as in the standard Dugdale approach. The main purposes of this article are to show, firstly, that this approximate representation of the plastic zone is reasonably accurate and, secondly, that the main interaction between the major crack and the MSD damage comes about through plastic yielding. That is, it will be shown that the reduction of the average yield stress brought about by the damage is the main cause of the reduction of residual strength arising in the interaction between damage and a major crack.

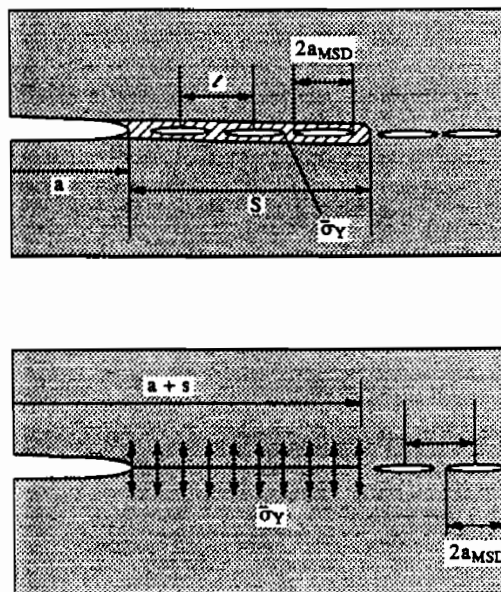


Fig. 2. Weakening of the sheet due to the micro-cracks: (a) a schematic illustration of the plastic zone extending from the tip of the major crack in the presence of micro-cracks. The zone engulfs several ligaments; (b) weakening as modeled by an average yield stress in the plastic zone (modified Dugdale model)

### Approximate representation of the micro-cracks outside of the plastic zone

The effect of a micro-crack lying in the elastic portion of the sheet on a major crack can be accurately approximated by replacing the micro-crack by a dislocation doublet and choosing the amplitude of the doublet such that the normal stress acting on the doublet center vanishes. Similar analytical approximations to model the effect of a micro-crack on a macro-crack, which have been developed and exploited by various workers, are discussed in the review article by Kachanov (1993). This approximation technique significantly reduces the numerical computation needed to solve the interaction problem. Moreover, it will be seen that the effects of the micro-cracks in the elastic portions of the sheet are relatively unimportant and, in fact, could be neglected with little error. Several criteria can be invoked to specify the relationship between the length of the micro-crack,  $2a_{\text{MSD}}$ , and the distance  $d$  separating the two equal and opposite dislocations in the doublet pair. A natural criterion is to choose  $d$  such that the increase in compliance brought about by equally spaced doublets along an infinite line (see Fig. 3) is identical to that caused by micro-cracks of length  $2a_{\text{MSD}}$  spaced the same way. The latter problem has been solved by Koiter (1959). The relation between  $d$  and  $a_{\text{MSD}}$ , such that the two problems have an identical increase in compliance, is plotted in Fig. 3. It can be seen that the spacing  $d$  separating the dislocations in the doublet pair is very close to the micro-crack length  $2a_{\text{MSD}}$ , and this is the choice that has been made in this paper. Thus, each micro-crack along the line of the major crack which is not engulfed by the Dugdale plastic zone will be represented by a dislocation doublet with spacing  $d = 2a_{\text{MSD}}$  and by an amplitude which is one of the unknowns in the problem. For each unknown amplitude, a condition is imposed that the resultant normal traction acting at the center of the doublet vanishes. For the elastic version of the problem in Fig. 1(a) with a single micro-crack interacting with a major crack, the stress intensity factor of the nearest main crack tip from this approach has been checked against the known solution to this problem and the approximate approach is found to be accurate.

### Representation of tear strap attachment

The rivet forces that transfer loads between the strap and the sheet may be computed by assuming displacement compatibility between the strap and the rivet at the attachment points. The concentrated force is assumed to be applied to the sheet at the center of the rivet, but the displacement of the sheet in the direction parallel to the strap,  $v$ , is taken as the average around a circular loop of radius  $R$  centered at the rivet center. This is a somewhat simpler procedure to implement than that used, for example, by Bloom and Sanders (1966) who took the rivets to be "rigid inserts" of radius  $R$ . Comparisons of the present method with that of Bloom and Sanders (1966) on some representative elastic problems indicated that the differences are typically less than 1% for the stress intensity factor of a major crack.

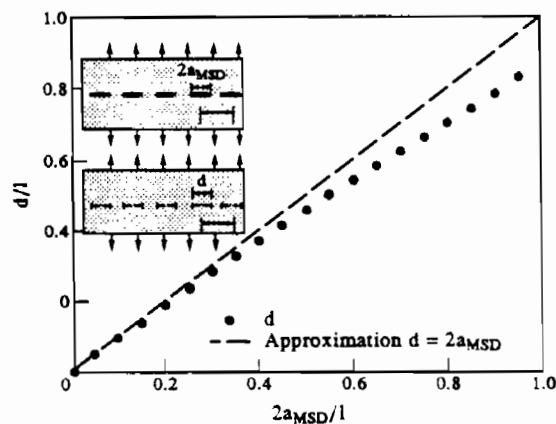


Fig. 3. The separation between dislocations in doublet pair  $d$ , and micro-crack length  $2a_{\text{MSD}}$ , for equal change in lap joint compliance for a row of cracks.

## THE COMPUTATIONAL MODEL

The computational set-up is now described. The five sub-solutions needed in the construction of the full solution are displayed pictorially in Fig. 4. Analytical representations for each of these sub-solutions can be obtained using complex variable methods; in the interest of brevity, they will not be given in this paper. All five sub-solutions are needed in constructing the elastic-plastic solution to the problem with tear straps, but problem C is not needed for the problem without tear straps. In the linear elastic analysis, there is no Dugdale zone (i.e.  $s = 0$ ), the half-length of the major crack is  $a$  and problem E is not needed.

In the linear elastic approach, the analysis provides the mode I stress intensity factor  $K$  of the main crack as a function of the applied stress  $\sigma$ , with allowance for tear strap yielding if that occurs. Then, imposition of the  $K = K_c$  gives the critical applied stress  $\sigma_c$  at which major crack advance occurs. For the elastic-plastic problem, the length of the Dugdale zone at each end of the major crack is denoted by  $s$ , and the reduced average yield stress  $\bar{\sigma}_Y$  acts along the line cut extended ahead of the major crack tip. The plastic zone length  $s$  is an unknown in the problem and must be chosen such that the normal stress acting across the line just ahead of the zone merges continuously with, and falls below,  $\bar{\sigma}_Y$ . The condition for continuity of the normal stress is the well-known requirement that the amplitude of the inverse square root stress singularity at the end of the zone must vanish. In the elastic-plastic approach, the analysis gives the relation between  $\delta_c$  and  $\sigma$ : the critical applied stress  $\sigma_c$  is obtained by imposing  $\delta_c = \delta_c^c$ .

The set-up of the computational model will be described for the elastic-plastic approach to the more complicated problem with tear straps. The set-up for the other problems will be evident. For the moment, assume that the stress everywhere in the tear strap falls below the tear strap yield stress  $\sigma_Y^{\text{strap}}$ . The tear straps are of width  $w$  and the same thickness  $t$  as the sheet. They are assumed to be riveted to the sheet with rivets of radius  $R$  spaced a distance  $h$  apart, as shown in Fig. 1(b) (bonded tear straps can be accommodated in an approximate manner within the present approach by taking the rivet spacing  $h$  to be sufficiently small). For a specified value of  $s$  and a given applied stress  $\sigma$ , the solution is constructed using linear superposition of the sub-solutions of Fig. 4. The condition for determining  $s$  will be discussed later. The unknowns are the  $N$  amplitudes  $b_i$  of the dislocation doublets centered at each of the micro-crack centers outside the plastic zone and the  $M$  forces  $P_i$  exerted by the tear straps on the sheet through the rivets. Double symmetry with respect to the origin at the center of the major crack is preserved. Only doublets lying to the right, and rivet forces to the upper right, of the major crack need be considered. The  $M + N$  equations for these unknowns are as follows. There are  $N$  equations corresponding to the condition that the net normal stress (summed over all the contributions) must vanish at each of the doublet centers. Equilibrium of the tear strap at each of the  $M$  tear strap rivets supplies the remaining equations. At rivets 2 through  $M - 1$ , equilibrium requires that

$$v_{i+1} - 2v_i + v_{i-1} = -hP_i / (Et w) \quad (3)$$

where  $v_i$  is the vertical displacement in the sheet at the  $i$ th tear strap rivet, as defined earlier. Equation (3) for  $i = 1$  applies with  $v_0$  replaced by  $-v_1$ , i.e.

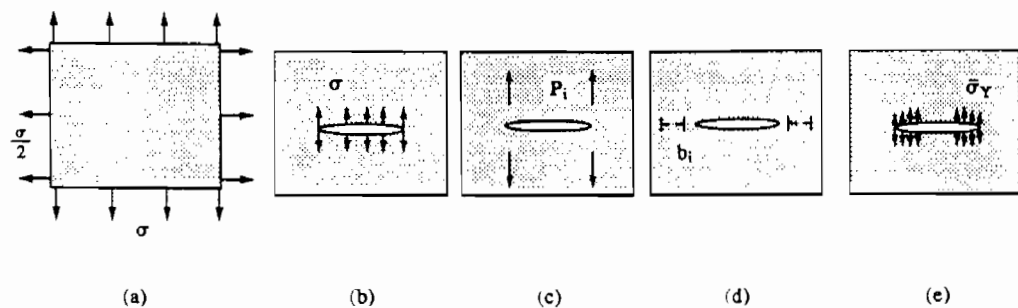


Fig. 4. The five sub-problems needed to analyse the cracked stiffened sheet in the presence of MSD.

$$v_2 - 3v_1 = -hP_1/(EtW). \quad (4)$$

The remote stress in the strap is  $\sigma$  and thus the equation for the top tear strap rivet for  $i = M$  is

$$v_M - v_{M-1} = hP_M/(EtW) + h\sigma/E. \quad (5)$$

The  $v_i$  in eqns (3)–(5) are expressed in terms of the unknowns,  $P_i$  and  $b_i$ , leading to a total of  $M+N$  equations and an equal number of unknowns.

For an arbitrarily specified value of  $s$ , the stresses at the end of the Dugdale zone at  $x = a+s$  will be unbounded with an inverse square root singular behavior, as discussed before. The condition of a zero amplitude of the inverse square root singularity at  $x = a+s$ , from all contributions supplies the equation relating  $s$  to  $\sigma$ . This condition is nonlinear in  $s$  but linear in  $\sigma$  and the other  $M+N$  unknowns. An effective procedure to generate numerical results takes  $s$  as specified and uses the condition as an extra linear equation to compute  $\sigma$  along with the other  $M+N$  unknowns. Once these have been determined, all other quantities of interest can be computed, including the stress in the segments of the tear strap between the rivets and the crack tip opening displacement  $\delta_i$ . The critical value  $\sigma_c$  is that value of  $\sigma$  such that  $\delta_i = \delta_i^*$ , corresponding to meeting the condition for advance of the major crack.

The above set of equations is modified if the stress in any segment of the tear strap reaches the yield stress  $\sigma_Y^{\text{strap}}$ . The numerical solutions show that yield is only reached in the segment of strap spanning the major crack line, i.e. the segment below tear strap rivet # 1. In the present paper, the strap is modeled as being elastic-perfectly plastic. When the segment spanning the major crack yields, the force in that segment is  $\sigma_Y^{\text{strap}}tW$  and eqn (4) must be replaced by

$$v_2 - v_1 = -hP_1/(EtW) + \sigma_Y^{\text{strap}}h/E. \quad (6)$$

otherwise, the procedure described above still applies. The strain in the yielded segment is computed using  $\epsilon = 2v_1/h$ ; consistency requires  $\epsilon > \sigma_Y^{\text{strap}}/E$ . A condition for failure of the strap could be prescribed, but that will not be done in the numerical examples discussed in this paper. Instead, the strap is allowed to yield, and results for the strain in the strap at  $\sigma_c$  will be presented. It will be seen that the onset of tear strap yielding does not usually coincide with the onset of major crack advance and, therefore, should not be used as a criterion for determining  $\sigma_c$ .

#### ASSESSMENT OF MODIFIED DUGDALE MODEL

The central idea underlying the modified Dugdale model is the use of the reduced average yield stress  $\bar{\sigma}_Y$  to characterize yielding ahead of the major crack. The reduced yield stress defined in eqn (2) reflects the weakening of the sheet material associated with damage due to small cracks. This approach can only be justified when the plastic zone encompasses enough small cracks to warrant the "smearing out" of their influence in this manner. The accuracy of the modified approach will be demonstrated by the following examples.

Consider the unstiffened sheet shown in Fig. 2 containing a major crack and the small crack damage. The approach described in the previous section has been applied to this problem; it is depicted in Fig. 2(b) under the heading of the modified Dugdale model. For comparison, to establish accuracy, we have also carried out some calculations using an "exact" Dugdale formulation, which is depicted in Fig. 2(a). In the exact version, zero traction conditions are satisfied along the line of the small cracks and the full sheet yield stress  $\sigma_Y$  is applied on the ligaments and portions of the ligaments, between the cracks where yielding occurs. The length of the plastic zone,  $s$ , is an unknown which must be determined from the usual condition that the stresses are bounded just ahead of the zone. Thus, the modified model includes the effect of the small cracks in the plastic zone only

through the reduced yield stress, while the "exact" model treats the small cracks as discrete entities in the zone. Both models account for the small cracks outside the plastic zone using the doublet approximation, which is accurate for this purpose. In the limit when the damage parameter  $D_{MSD}$ , defined in eqn (2), is zero, both models reduce to the classical Dugdale model.

In this example and in others considered later, the sheet material will be assigned properties representative of aluminum 2024-T3 with  $E = 69.7$  GPa (10.1 Msi),  $\nu = 0.33$  and  $\sigma_Y = 345$  MPa (50 ksi). The skin thickness, which does not enter in the examples of this section, is taken to be 1.02 mm (0.04 inches). The fracture toughness,  $K_c$ , of the material with this thickness is reported by Samavedam *et al.* (1992) to be about 165 MPa/m<sup>1/2</sup> (150 ksi/inch<sup>1/2</sup>) (resistance curve behavior will not be taken into account in this paper). However, this value is higher than that used by others for this material (e.g Hoysan and Sinclair, 1993), and thus in some examples the value  $K_c = 110$  MPa/m<sup>1/2</sup> (100 ksi/inch<sup>1/2</sup>) will also be used in carrying out calculations. The associated critical crack opening displacements (1) are

$$\begin{aligned}\delta_i^c &= 1.130 \text{ mm (0.045 inches) for } K_c = 150 \text{ ksi/inch}^{1/2} \\ \delta_i^c &= 0.503 \text{ mm (0.020 inches) for } K_c = 100 \text{ ksi/inch}^{1/2}.\end{aligned}\quad (7)$$

For reference, it is noted that the small scale yielding estimate of the plastic zone length of the undamaged sheet at the onset of crack advance is

$$\begin{aligned}s &= (\pi/8)(K_c/\sigma_Y)^2 \\ &= 9.0 \text{ cm (3.5 inches) for } K_c = 150 \text{ ksi/inch}^{1/2} \\ &= 4.0 \text{ cm (1.6 inches) for } K_c = 100 \text{ ksi/inch}^{1/2}.\end{aligned}\quad (8)$$

The spacing between the centers of the small cracks is taken to be  $l = 2.54$  cm (1 inch) in all the examples in this paper.

An example showing the relationship between the normalized applied stress  $\sigma/\sigma_Y$  and the plastic zone length  $s$  is shown in Fig. 5(a), and the corresponding relationship between the normalized crack tip opening displacement  $\delta_i/\delta_i^c$  and  $s$  is shown in Fig. 5(b), in each case for  $a = 13.7$  cm (5.4 inch) and  $2a_{MSD} = 1.27$  cm (0.5 inch) corresponding to  $D_{MSD} = 0.5$ . (Here  $\delta_i^c = 1.13$  mm;  $\delta_i^c$  is used as a normalizing factor in this plot. It does not otherwise play a role until the solution is used to predict  $\sigma_c$  in Fig. 6.) The dashed-line curves in each of these figures represent the results of the modified model. The solid points in these figures are the predictions of the exact model corresponding to the points where the end of the plastic zone extends exactly half way across the ligament connecting the micro-crack just outside the zone. The full details of the exact model as the plastic zone engulfs each ligament need not be displayed. The results of Fig. 5 show that the relative error of the modified model decreases as the applied stress increases and the plastic zone engulfs more and more of the small cracks. The accuracy of the modified model is even more evident when the predictions of the critical stress from the two models are compared. For this purpose the condition  $\delta_i = \delta_i^c$  is imposed on each of the solutions. Figure 6 displays  $\sigma_c/\sigma_Y$  as a function of  $a$  for four levels of damage, in (a) for the tougher material with  $\delta_i^c = 1.130$  mm and in (b) for the other material with  $\delta_i^c = 0.503$  mm. The predictions for the exact model, calculated by interpolating between points such as those in Fig. 5, are shown as solid points and predictions from the modified model are shown as dashed-line curves. The agreement between the two models is better for the tougher material since it has the large plastic zone size, but in both cases the agreement is very good with the modified model consistently giving the lower estimate. It can be concluded that the use of an average yield stress reduced to account for small crack damage is an effective way to model the effect of the damage on the plastic yielding behavior even when the plastic zone length engulfs only about two small



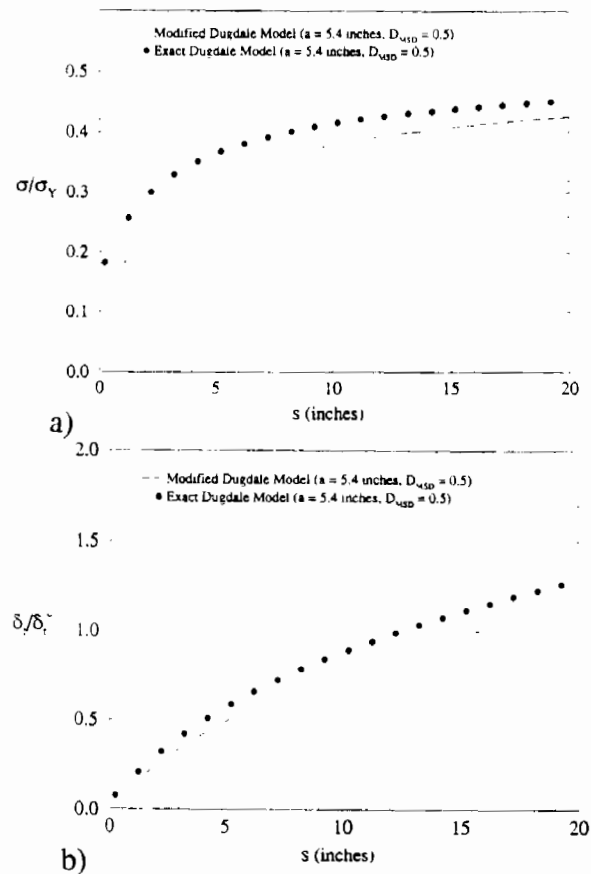


Fig. 5. (a) Normalized applied stress as a function of the plastic zone length for an unstiffened sheet; (b) normalized crack tip opening as a function of the plastic zone length for an unstiffened sheet.  $2a = 10.8$  inches (27.4 cm),  $D_{MSD} = 0.5$ ,  $\sigma_Y = 50$  ksi (345 MPa) and  $\delta_i^c = 0.045$  inches (1.13 mm).

cracks, as in the case of the less tough material in eqn (8). The modified zone approximation will be used in computing the examples in the remainder of the paper.

#### ELASTIC ANALYSIS VS THE MODIFIED DUGDALE MODEL FOR THE UNSTIFFENED SHEET AND A SIMPLE MODIFICATION OF LEFM

To illustrate how important it is to account for the interaction between plastic yielding and damage, the results of Fig. 6(a) obtained from the modified zone model are displayed in Fig. 7 along with predictions calculated by the elastic approach. These results are for the tougher of the two sheet materials, and the comparison for the less tough material is similar. The elastic results were computed as described earlier accounting for the elastic interaction between the small cracks and the major crack with no plastic yielding. The criterion  $K = K_c = 165$  MPa  $m^{1/2}$  (150 ksi  $inch^{1/2}$ ) was imposed on the elastic solution to give  $\sigma_c$ . In Fig. 7, for presentation purposes,  $\sigma_c$  has been normalized by  $\sigma_Y$  even though it does not play a role in the elastic solution. There are two important conclusions which can be drawn from the comparisons in Fig. 7.

The difference between the two models for the undamaged sheet (i.e. the sheet with a major crack but no small cracks) is not significant, except when the major crack is relatively short so that the plastic zone becomes large compared to the crack length. In the case of the undamaged sheet ( $D_{MSD} = 0$ ), the modified model is identical to the standard Dugdale model, and the elastic prediction is the same as that of LEFM for a crack of half-length  $a$  in an infinite sheet. For cracks with half-lengths greater than about 13–25 cm (5–10 inches) in this sheet material, the LEFM approach suffices for undamaged sheet material.

By contrast, the elastic predictions completely fail to capture the effect of the small crack damage on the reduction of the critical stress  $\sigma_c$ . For a damage level as large as

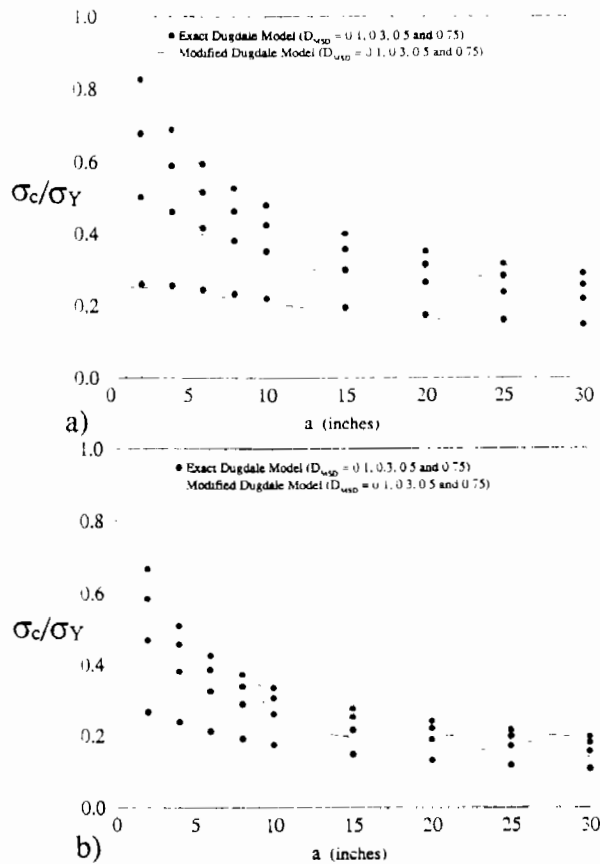


Fig. 6. Residual strength curves for an unstiffened sheet as given by the modified and "exact" Dugdale models, respectively: (a)  $\delta_0^* = 0.045$  inches (1.14 mm), (b)  $\delta_0^* = 0.020$  inches (0.50 mm).

$D_{MSD} = 0.5$ , there is hardly any reduction in the critical stress according to the elastic predictions, while the modified Dugdale model predicts a reduction of about 30%, and even larger when the major crack is less than about 25 cm (10 inches). This example makes clear that, as has already been emphasized, the main effect of the damage is the reduced strength of the sheet in the plastic zone and not its effect on the sheet in the elastic region.

These two observations, together with the demonstrated success of the use of the reduced yield stress  $\bar{\sigma}_Y$  to model the effect of damage, suggest a potentially useful way to modify conventional LEFM to account for the effect of damage on the crack advance criterion for a major crack, as long as the plastic zone is sufficiently short compared to the length of the major crack. In small scale yielding, the plane stress relation between the crack tip opening displacement and the stress intensity factor for the undamaged sheet is

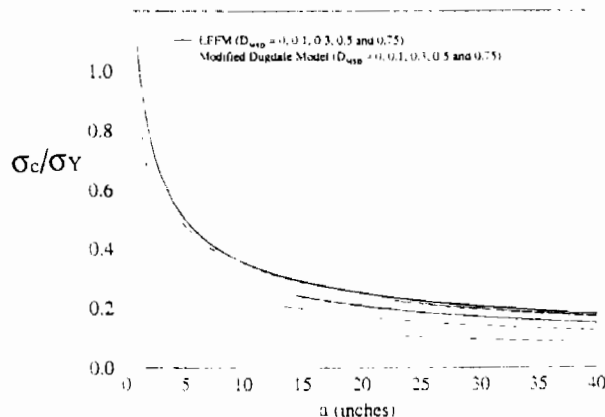


Fig. 7. Residual strength curves for an unstiffened sheet as given by a linear elastic fracture mechanics analysis (LEFM) and the modified Dugdale model for  $D_{MSD} = 0, 0.1, 0.3, 0.5$  and  $0.75$ .  $K_{IC} = 150$  ksi $\sqrt{\text{in}}$  (165 MPa $\sqrt{\text{m}}$ ),  $\delta_0^* = 0.045$  inches (1.14 mm).

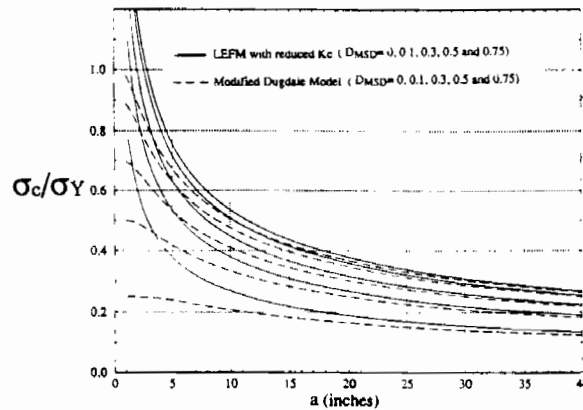


Fig. 8. Residual strength curve for an unstiffened sheet as given by a linear elastic fracture analysis with reduced fracture toughness due to micro-cracks ( $\bar{K}_c = K_{c\sqrt{1-D_{MSD}}}$ ) and the modified Dugdale model for  $D_{MSD} = 0, 0.1, 0.3, 0.5$  and  $0.75$ .  $K_c = 150 \text{ ksi}\sqrt{\text{inch}}$  ( $165 \text{ MPa}\sqrt{\text{m}}$ ),  $\delta_i^c = 0.045 \text{ inches}$  ( $1.14 \text{ mm}$ ).

$\delta_i = K^2 (E\sigma_Y)$ . If the spacing between the small cracks representing the damage is small compared to the plastic zone length, and at the same time the plastic zone is sufficiently short compared to the length of the major crack, then one can regard the situation as a small scale yielding problem with a modified yield stress  $\bar{\sigma}_Y$ , such that  $\delta_i = K^2/(E\bar{\sigma}_Y)$ . Retaining the criterion  $\delta_i = \delta_i^c$ , one is immediately led to a modified critical stress intensity factor associated with crack advance:

$$\begin{aligned} \bar{K}_c &= \sqrt{E\bar{\sigma}_Y\delta_i^c} \\ &= \sqrt{\frac{\bar{\sigma}_Y}{\sigma_Y}} K_c = \sqrt{1-D_{MSD}} K_c. \end{aligned} \quad (9)$$

Thus, the proposal is to use conventional LEFM with no account taken of the small cracks representing the damage other than their effect on the modified yield stress in eqn (9). Instead of the criterion  $K = K_c$ , it is proposed to use  $K = \bar{K}_c$ . For the major crack of half-length in the infinite sheet, the equation for the critical stress according to this simple proposal is just  $\sigma_c\sqrt{\pi a} = \bar{K}_c$ . The predictions of this simple formula for the tougher of the two sheet materials are plotted in Fig. 8, where they are compared with the results from Fig. 7 based on the modified Dugdale approach. As conjectured above, as the crack becomes longer the proposed modification of LEFM gets gradually more accurate, and for major crack half-lengths greater than about 10–15 inches, it gives sufficient accuracy in this application. For short major cracks, large scale yielding occurs and the modified LEFM approach significantly overestimates the residual strength of the sheet. Comparisons for the less tough of the sheet materials show similar good agreement. From eqns (2) and (9), one finds by this proposal the simple formula for the relationship of the critical stress of the damaged sheet to that of the undamaged sheet

$$\frac{(\sigma_c)_{\text{damaged}}}{(\sigma_c)_{\text{undamaged}}} = \sqrt{\frac{\bar{\sigma}_Y}{\sigma_Y}} = \sqrt{1-D_{MSD}}. \quad (10)$$

The strength reduction implied by this formula applies to all cases where small scale yielding holds in the sense described above. For the aluminum sheet materials this requires that the major half-crack length be greater than about 10 inches.

There is considerable appeal in being able to retain the framework of conventional LEFM for analysing the residual strength of aircraft fuselages containing major cracks. The proposal made here would make this possible. Its application to an example for a reinforced sheet will be discussed below where a potential limitation will emerge.

We remark in passing, that a criterion of major crack advance based on the attainment of complete plastic yielding of the ligament connecting the major crack tip with the closest rivet crack is not likely to give realistic predictions when configurations have major crack sizes and rivet spacings typical of aircraft lap joints. Application of this criterion to the present problems would substantially underestimate the residual strength. This is evident, for example, from the fact that the smallest plastic zones at major crack advance are about 2 inches long for the less tough of the two materials and 4 inches long for the tougher material. In some instances the plastic zones are even longer at the onset of major crack advance.

#### REINFORCED SHEET CONTAINING A MAJOR CRACK

An infinite flat sheet stiffened by two tear straps spaced by a distance  $2L = 20$  inches (50.8 cm) is considered. The straps have the same thickness as the sheet, width  $w = 2$  inches (5.08 cm) unless otherwise stated, and are riveted to the sheet by rivets of radius  $R = 0.08$  inch (0.203 cm) spaced a distance  $h = 1$  inch (2.54 cm) apart. Twenty rivets in the upper right hand quadrant were used in the analysis. The inclusion of more rivets was found to have no influence on the solution. The tear strap material is taken to be aluminum 7075-T6 with a yield stress  $\sigma_Y^{\text{tear strap}} = 70$  ksi (482 MPa). The sheet toughness in these examples will be taken to be  $K_c = 100$  ksi/inch<sup>1.2</sup> (110 MPa/m<sup>1.2</sup>), and thus the second of the critical crack opening displacement values in eqn (7) apply in the elastic-plastic modeling. In this study, the tear straps will be considered to be elastic-perfectly plastic. As discussed earlier, they will be allowed to yield and strain, but not to fail. The strain in the tear strap will be plotted along with the residual stress curves.

The two sets of plots in Fig. 9 show the predictions of the approach which treat the sheet as being elastic but allows yielding in the tear strap. The corresponding predictions

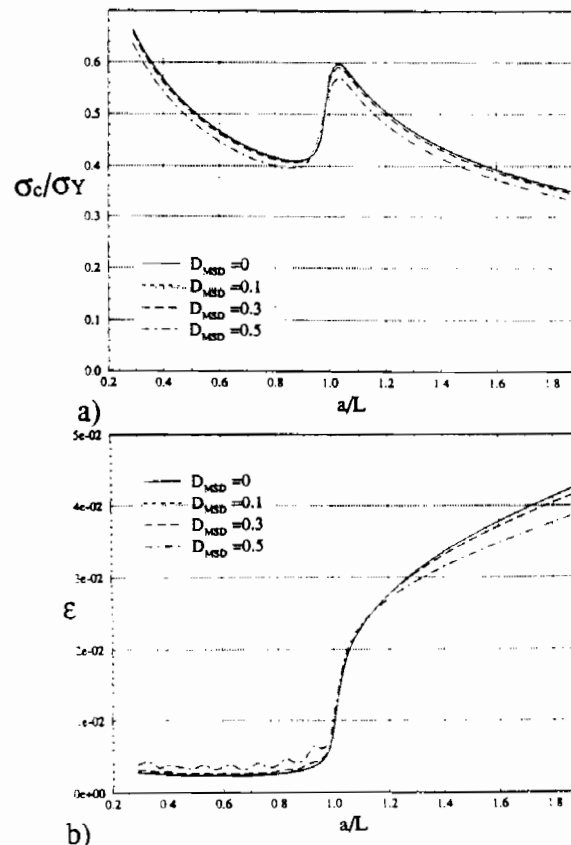


Fig. 9. (a) Residual strength curve for a stiffened sheet as given by a linear elastic fracture model.  $K_c = 110$  ksi $\sqrt{\text{inch}}$  (110 MPa $\sqrt{\text{m}}$ ), for  $D_{\text{VSD}} = 0, 0.1, 0.3$  and  $0.5$ ; (b) maximum strain levels in tear strap associated with the residual strength levels in (a).

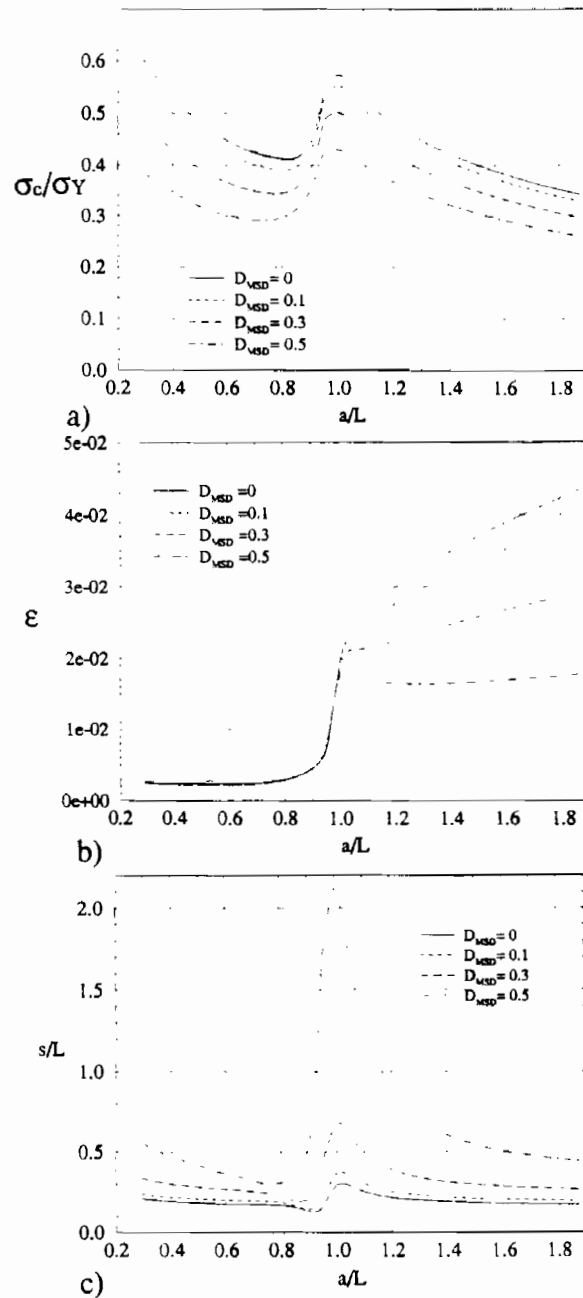


Fig. 10. (a) Residual strength curve for a stiffened sheet as given by the modified Dugdale model  $\delta_1^* = 0.020$  inches (0.51 mm) for  $D_{MSD} = 0, 0.1, 0.3$  and  $0.5$ ; (b) maximum strain levels in tear strap associated with the residual strength levels in (a); (c) Dugdale zone lengths associated with the residual strength levels in (a).

for the modified Dugdale approach are shown in Fig. 10. The residual strength curves predicted by the elastic analysis (with plastic yielding of the tear strap) in Fig. 9(a) show very little degradation of strength due to damage, similar to what was observed for the unstiffened sheet. Accounting for plastic yielding through the modified Dugdale approach indicates a fairly strong reduction in residual strength due to damage, as was also the case for the unstiffened sheet. Note again, however, that the predictions of the two approaches for the undamaged sheet are not significantly different. In other words, an LEM approach (accounting for tear strap yielding) is adequate for predicting residual strength of this problem when there is no small crack damage, but cannot be used to predict the effect of damage.

The tensile strain  $\epsilon$  in the tear strap in the segment which spans the line of the cracks (i.e. at  $y = 0$ ) at the point when  $\sigma_c$  is attained, is plotted in Figs 9(b) and 10(b) for each of

the two approaches. The strain at the onset of yield is  $\varepsilon_Y = 0.007$  and it is seen that the tear straps remain elastic at  $\sigma_c$  for half-crack lengths  $a$  which are less than about  $0.9L$  for each of the models. For major cracks longer than this, the tear strap yields prior to attainment of the  $\sigma_c$  and undergoes plastic straining. It is important to note that the strain levels in the strap at  $\sigma_c$  are not unduly large, values 3–5 times  $\varepsilon_Y$  are typical as the crack extends under the tear strap. In general though, the possibility of tear strap failure should be incorporated into the model. Figure 10(c) displays the normalized length of the plastic zone,  $s/L$ , at  $\sigma_c$  according to the modified Dugdale model. In particular, it can be noted that the plastic zone in the undamaged sheet is never more than about  $L/3$ , and this is why the two approaches give similar predictions for this case. For the highest damage level ( $D_{MSD} = 0.5$ ), the plastic zone becomes very large when the major crack tip is in the vicinity of the tear strap, and large scale yielding prevails. In general, the greater the damage, the greater the extent of the plastic zone. This remark clearly has significance to application of the simple modified LEM approach proposed in the section above.

The simple modified LEM approach based on the criterion  $K = \bar{K}_c$  has been applied to this problem, and the predicted residual strength curves are plotted in Fig. 11 for  $D_{MSD} = 0$  and 0.5. In applying this method, we have used the modified toughness for the damaged sheet given by eqn (9), together with an elastic analysis for  $K$  which accounts for tear strap yielding in the same manner as described for the other two approaches. In other words,  $K$  is computed by the procedure specified for the undamaged elastic sheet. The prediction based on the simple formula (10) is also included in this figure, where  $(\sigma_c)_{undamaged}$  is the LEM prediction (i.e. the upper dashed curve in Fig. 11). For major half-crack lengths  $a$  less than about  $0.9L$ , the strap remains elastic for applied stresses up to  $\sigma_c$  [cf. Fig. 9(b)], and thus it is a straightforward matter to show that the simple formula (10) applies rigorously in this range for the modified LEM approach. At longer major crack lengths, eqn (10) does not apply to the modified LEM because the nonlinear behavior of the tear strap must be taken into account; these portions of the curves have been computed numerically. It is evident that the simple modification of the LEM approach provides a good approximation to the predictions of the modified Dugdale model for major cracks of half-length between about  $0.5L$  and  $0.8L$ . For major cracks of half-length  $a$  approximately equal to  $L$ , the simple modification of LEM seriously underestimates the reduction in  $\sigma_c$  due to damage. This, of course, is an important range of crack lengths since the peak "arrest" strength lies in this range. The reason for the failure of the modified LEM is related to the fact, mentioned in connection with Fig. 10(c), that, at levels of damage  $D_{MSD}$  as large as 0.25 and 0.5, large scale yielding prevails. The lowering of the effective yield stress of the Dugdale zone results in a significant increase in the plastic zone size, thereby invalidating the use of LEM with a damage-reduced toughness in this range of crack lengths. Curiously, the reduction predicted by eqn (10) in this range remains reasonably accurate, even though it is being applied outside its intended range of validity.

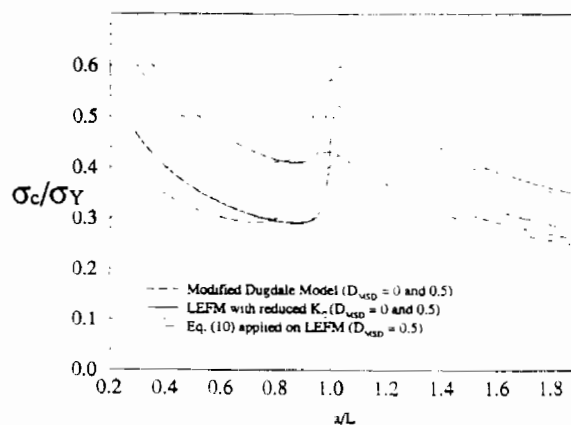


Fig. 11 Residual strength curve as given by LEM with reduced fracture toughness ( $\bar{K}_c = K_{c0} \sqrt{1 - D_{MSD}}$ ) and the modified Dugdale model for  $D_{MSD} = 0$  and 0.5 for a stiffened sheet. The prediction of eqn (10) is also shown for  $D_{MSD} = 0.5$ .

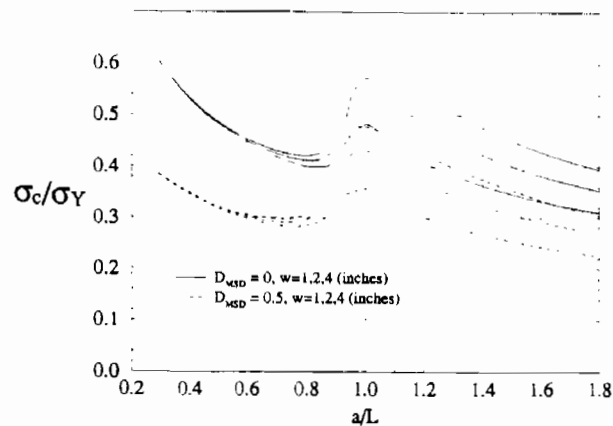


Fig. 12. Residual strength curves as given by the modified Dugdale model for three strap widths,  $w = 1, 2$  and 4 inches (2.54, 5.08 and 10.2 cm), and two damage levels  $D_{\text{MSD}} = 0$  and 0.5.

As a final example, the modified Dugdale model will be used to show the effect of tear strap width on residual strength behavior. In this example, the effect of doubling ( $w = 4$  inches) and halving ( $w = 1$  inch) the width from what was taken in the previous example ( $w = 2$  inches) will be analysed. Otherwise, the parameters characterizing the problem are unchanged. Figure 12 shows curves of  $\sigma_c$  as a function of  $a$  for each of the three widths for both the undamaged case ( $D_{\text{MSD}} = 0$ ) and the case with  $D_{\text{MSD}} = 0.5$ . The curves for  $w = 2$  inches are the same as those in Fig. 10(a). The tear strap width has relatively little influence for half-crack lengths less than about  $0.9L$ , since no yielding occurs, but becomes significant for longer cracks. Again, the simple formula (10) captures the effect of damage reasonably accurately for all crack lengths up to and including the peak residual strength, which occurs when  $a$  is about equal to  $L$ .

#### SUMMARY REMARKS

For material properties typical of those of an airplane fuselage and idealized to be elastic-perfectly plastic, this paper has considered the effect of damage on the residual strength of a flat sheet containing a representative major crack. The damage is represented as small cracks spaced at intervals typical of lap joint rivet spacing. The main effect of the damage is found to be the reduction of the average yield strength of the sheet in the plastic zone. The presence of the damage in the elastically deforming portions of the sheet is relatively unimportant. By way of example, the paper first demonstrates that a modified Dugdale approach is accurate wherein the small crack damage in the plastic zone can be accounted for by a reduced average yield stress  $\bar{\sigma}_Y$ , where  $\bar{\sigma}_Y = \sigma_Y (1 - D_{\text{MSD}})$ , with  $D_{\text{MSD}}$  as the damage measure defined in eqn (2) reflecting the fractional reduction in ligament area. The main implication of this finding is that an all important aspect of MSD damage is its role in reducing the yield strength of the lap joint. Then it was shown that under restricted conditions (i.e. a plastic zone which is small compared to the length of the major crack) an even simpler approach could be employed which involves a modification of LEFM based on a damage-reduced toughness  $\bar{K}_{Ic}$  given in eqn (9) (it is important in this approach to account for tear strap yielding). When applicable, the modified LEFM approach has the substantial attraction that it involves essentially no additional complications from what must be considered in a fracture analysis of the undamaged configuration. In particular, when no tear strap yielding occurs, this approach gives the elementary, but insightful, result (10). For the examples considered here, eqn (10) even gives a reasonably accurate prediction effect of damage on the peak value of  $\sigma_c$ , which is attained when the major crack has length about equal to the tear strap spacing and which involves some tear strap yielding. In other words,  $\bar{\sigma}_Y / \sigma_Y$  gives a reasonable measure of the ratio of the residual strength of the problem with MSD damage to that without MSD damage. This result again emphasizes the importance of understanding, or measuring, the effect of damage on the yield strength of the joint.

Whether it be for the modified Dugdale approach or the even simpler modified LEFM approach, more work needs to be done to characterize the damage in a lap joint and to relate that damage to a reduced average yield stress or a reduced fracture toughness. Consideration should be given to strain hardening of the materials of the sheet and the tear straps and to shell curvature effects. Crack growth resistance of the sheet material should also be taken into account. Both of these effects are considered in the modeling of Newman *et al.* (1993). In addition to being computationally simpler, the advantage of each of the two approaches presented in this paper is that they allow a decoupling of the analysis (or the experimental measurement) of the effect of damage on the joint response from the assessment of residual strength in the presence of a major crack. This decoupling is most apparent for the modified LEFM approach in that damage comes in only through the reduced fracture toughness  $\bar{K}_c$ . For the modified Dugdale approach, damage influences the average effective yield stress  $\bar{\sigma}_Y$ .

*Acknowledgements*—This work was supported in part by the Federal Aeronautics Administration by FAA Grant No. 92-G-009 and in part by the Division of Applied Sciences, Harvard University. KFN would also like to acknowledge partial support from Blanceflor Boncompagnie-Ludovisi nee Bildt Foundation for the period he was at Harvard, and to the Swedish National Board for Industrial and Technical Development since he returned to work at the FFA in Sweden.

#### REFERENCES

- Bloom, J. and Sanders, J. L. (1966). The effect of a riveted stringer on the stress in a cracked sheet. *J. Appl. Mech.* **33**, 561–570.
- Hoysan, S. F. and Sinclair, G. B. (1993). On the variability of fracture toughness. *Int. J. Fract.* **60**, R43–R49.
- Kachanov, M. (1993). Elastic solids with many cracks and related problems. In *Advances in Applied Mechanics* (Edited by J. W. Hutchinson and T. W. Wu), Vol. 30, pp. 259–428. Academic Press, New York.
- Koiter, W. T. (1959). An infinite row of collinear cracks in an infinite elastic sheet. *Ing. Archiv.* **28**, 168–172.
- Newman, J. C., Dawicke, D. S., Sutton, M. A. and Bigelow, C. A. (1993). A fracture criterion for widespread cracking in thin-sheet aluminum alloys. *17th Symp. Int. Comm. Aeronautical Fatigue*, Stockholm, Sweden.
- Park, J. H., Ogiso, T. and Atluri, S. N. (1992). Analysis of cracks in aging aircraft structures, with and without composite patch repairs. *Comput. Mech.* **10**, 169–201.
- Samavedam, G., Hoadly, D. and Thompson, D. (1992). Full scale testing and analysis of curved fuselage panels. Federal Aviation Administration, Department of Transportation, Report DOT-92-01.
- Swift, T. (1974). The effects of fastener flexibility and stiffener geometry on stress intensity in stiffened cracked sheet. In *Prospects of Fracture Mechanics*, pp. 419–436. Noordhoff International, Leyden, The Netherlands.
- Swift, T. (1986). Important considerations in commercial aircraft damage tolerance. *Int. J. Vehicle Des.* **7**, 264–287.
- Tong, P., Greif, R. and Chen, L. (1994). Residual strength of aircraft panels with multiple-site damage. *Comput. Mech.* **13**, 285–294.